HHS Public Access

Author manuscript

Pain. Author manuscript; available in PMC 2019 April 15.

Published in final edited form as:

Pain. 2011 August ; 152(8): 1766–1776. doi:10.1016/j.pain.2011.03.024.

P2X7 receptor-deficient mice are susceptible to bone cancer pain

Rikke Rie Hansen[a], **Christian K. Nielsen**[a], **Arafat Nasser**[a], **Stine I.M. Thomsen**[a], **Laura F. Eghorn**[a], **Yen Pham**[a], **Cecilia Schulenburg**[a], **Susanne Syberg**[b], **Ming Ding**[c], **Stanko S. Stojilkovic**[d], **Niklas R. Jorgensen**[b], and **Anne-Marie Heegaard**[a,*]

[a]Department of Pharmacology and Pharmacotherapy, Faculty of Pharmaceutical Sciences, Copenhagen University, Copenhagen, Denmark

[b]Center for Ageing and Osteoporosis, Research Centre Glostrup, Glostrup Hospital, Denmark

[c]Odense University Hospital, University of Southern Denmark, Odense, Denmark

[d]Eunice Kennedy Shriver National Institute of Child Health and Human Development, National Institutes of Health, Bethesda, Maryland, USA

Abstract

The purinergic P2X7 receptor is implicated in both neuropathic and inflammatory pain, and has been suggested as a possible target in pain treatment. However, the specific role of the P2X7 receptor in bone cancer pain is unknown. We demonstrated that BALB/cJ P2X7 receptor knockout (P2X7R KO) mice were susceptible to bone cancer pain and moreover had an earlier onset of pain-related behaviours compared with cancer-bearing, wild-type mice. Furthermore, acute treatment with the selective P2X7 receptor antagonist, A-438079, failed to alleviate pain-related behaviours in models of bone cancer pain with and without astrocyte activation (BALB/cJ or C3H mice inoculated with 4T1 mammary cancer cells or NCTC 2472 osteosarcoma cells, respectively), suggesting that astrocytic P2X7 receptors play a negligible role in bone cancer pain. The results support the hypothesis that bone cancer pain is a separate pain state compared with those of neuropathic and inflammatory pain. However, the recent discovery of a P2X7 receptor splice variant expressed in the knockout mice used for this study complicates the interpretation of the results. The P2X7 splice variant receptor was detected in the spinal cord but not in osteoclasts of the P2X7R KO mouse. Further experiments are needed to elucidate the exact role of the P2X7 receptors in bone cancer pain.

Pain-related behaviours had an earlier onset in bone cancer-bearing, P2X7 receptor-deficient mice, and treatment with A-438079 failed to alleviate pain-related behaviours.

Keywords

Bone cancer pain; P2X7 receptor; IL-1β

[*]Corresponding author. Address: Department of Pharmacology and Pharmacotherapy, Faculty of Pharmaceutical Sciences Universitetsparken 2, DK-2100 Copenhagen, Denmark. Tel.: +45 3533 6322; fax: +45 3533 6020. amhe@farma.ku.dk.

Conflict of interest statement

None of the authors report any conflict of interest.

1. Introduction

Bone cancer pain is the most common pain in cancer patients [35], and it can severely compromise the quality of life [10,35]. In particular, breakthrough pain and incident pain is difficult to control, and the need for strong opiods increases as the bone cancer evolves [1,36,52]. The current treatment options for cancer-related bone pain leave some patients without adequate pain relief and are associated with dose limiting side effects [1,36]; therefore, new therapeutic options are needed. At the cellular level, bone cancer pain has components of both inflammatory and neuropathic pain but it is not yet fully classified. The spinal cord neurochemical changes seen in a murine model of bone cancer pain are distinct from those in neuropathic and inflammatory pain [25,29], suggesting that bone cancer pain is a separate pain state [7,22]. One nociceptive pathway that has not been fully investigated in bone cancer pain is purinergic signalling.

ATP and other nucleotides are now regarded as neuromodulators, and their involvement in pain is well established [3,16]. ATP acts as an agonist for 2 classes of receptors: ligand gated ion channels, the P2X receptors, and G-protein-coupled P2Y receptors [39]. The P2X7 receptor, one of the P2X receptors implicated in nociceptive signalling, has some distinguishing features. It requires high concentrations of ATP for activation (>100μM), and upon prolonged ATP stimulation it is involved in the formation of pores that allow passage of large organic cations [39]. The implication of the P2X7 receptors in pain has been established in animal models of both neuropathic and inflammatory pain. Chessell et al. demonstrated that pain-related behaviours were absent in P2X7 receptor-deficient mice with neuropathic pain induced by partial nerve ligation, and that mechanical hypersensitivity was absent in inflammation induced by Complete Freund's adjuvant (CFA) [5]. In addition, several specific P2X7 receptor antagonists have proved effective in animal models of pain [27,28,34,37].

The P2X7 receptor has been hypothesized to be part of a common pathway in the central sensitization seen in chronic pain, as activation leads to the release of mature active interleukin-1β (IL-1β) [5,17,48], which in turn triggers release of other pronociceptive mediators, among others, nitric oxide synthase and cyclooxygenase-2 [14,44]. The P2X7 receptor has been suggested as a possible target in inflammatory and neuropathic pain, however the involvement of the P2X7 receptor in bone cancer pain is yet unknown. Here we show that P2X7 receptor-deficient mice are susceptible to bone cancer pain, and moreover that they have an earlier onset of pain-related behaviours compared with wild-type mice. Also acute treatment with the selective P2X7 receptor antagonist, A-438079, fails to alleviate bone cancer pain-related behaviours.

2. Methods

2.1. Experimental animals

BALB/cJ wild-type (WT) and P2X7 receptor knockout (P2X7R KO) mice were bred in-house. The BALB/cJ P2X7R KO mice had been generated from the C57BL/6 P2X7R KO mice [5] and backcrossed for more than 7 generations into BALB/cJ mice. BALB/cJ, C3H/

HeN, and C57BL/6 mice were purchased from Taconic (Tornbjerg, Denmark). Pfizer P2X7R KO C57BL/6 mice were obtained from the Faculty of Science, Copenhagen University (Copenhagen, Denmark).

All mice were 6 to 8weeks old, housed at a 12-hour light/dark cycle and allowed free access to water and standard diet. All experiments were approved by the Danish Animal Experiments Inspectorate and conducted according to the guidelines of the International Association for the Study of Pain [54].

2.2. Cell lines

4T1 mammary cancer cells were obtained from American Type Culture Collection (CRL-2539, ATCC; LGC Standards AB, Boras, Sweden). Cells were subcultured according to the manufacturer's instructions. Cultures were harvested with 0.25% trypsin-EDTA (Gibco Invitrogen, Taastrup, Denmark) and resuspended in 0.1M D-PBS for the cancer operation. NCTC clone 2472 was obtained from ATCC (CCL-11) and cultured in NCTC-135 medium (Sigma-Aldrich, Brondby, Denmark) supplemented with sodium hydrogencarbonate and 10% equine serum (Sigma-Aldrich, Brondby, Denmark). Cultures were harvested at approximately 70% confluence with 1.0mM EDTA in 0.1M D-PBS, and resuspended in 0.1M D-PBS for the cancer operation. All cells were kept on ice until implantation.

2.3. Animal studies in P2X7 receptor-deficient mice

BALB/cJ WT and P2X7R KO mice were subjected to either the bone cancer operation (n=12 and n=14, respectively) or a sham operation (n=11 and n=10, respectively). Limb use and weight bearing were assessed at a pretest and on days 7, 10, and 14 postoperation.

Neuropathic pain was induced by the spared nerve injury (SNI). BALB/cJ WT and P2X7R KO mice were either SNI (n=6 and n=9, respectively) or sham operated (n=4 and n=6, respectively). Mechanical allodynia and thermal hyperalgesia were assessed on days −2 and −1 preoperation and on days 1, 2, 3, 6, 9, 12, 16, and 21 postoperation.

2.4. A-438079 treatment

BALB/cJ mice were designated one of 3 treatment groups: (1) bone cancer operation and vehicle treatment; (2) bone cancer operation and A-438079 treatment; or (3) sham operation and vehicle treatment (n=12 in each group). Only cancer-bearing mice with a day 14 limb use score ≤3 were included in the drug test giving groups of n=6, n=6, and n=12, respectively. Day 14 postoperation limb use and weight bearing were assessed at a pretest and 30 minutes after administration of either A-438079 (300μmol/kg, s.c.) or vehicle (5% ethanol, 10% Tween80 and 85% saline). C3H/HeN mice were in parallel designated one of 3 treatment groups (n=12 in each group). The same inclusion criteria for drug test were applied giving groups of n=10, n=10, and n=12, respectively. Day 17 limb use and weight bearing were assessed at a pretest and at 30 and 60 minutes after administration of either A-438079 (300μmol/kg, s.c.) or vehicle.

A subgroup of BALB/cJ WT mice were subjected to formalin-induced pain. Thirty minutes before formalin injection, mice were administered either A-438079 (300μmol/kg in saline, s.c., n=5) or saline (n=6).

Naive BALB/cJ mice were tested in a Rotarod challenge to assess a possible effect of A-438079 (300μmol/kg, s.c., n=4) on motor coordination. Time to fall and acceleration at fall was determined 30 minutes after A-438079 administration. The mice served as internal controls and had before the drug administration undergone 3 training sessions.

2.5. Bone cancer operation

Bone cancer was induced as described previously [8,9] with few modifications. In brief, mice were anaesthetized with a mixture of hypnorm/dormicum (Pharmacy Services, Faculty of Life Sciences, Frederiksberg, Denmark and Roche, Hvidovre, Denmark; 1.25mg/mL midazolam, 2.5mg/mL fluanisone, and 0.079mg/mL fentanylcitrate; 6μL/g). An incision was made over the patella and the patella tendon and the distal medial part of vastus medialis were loosened. The medial collateral ligament was cut and patella pushed aside to expose the distal femoral epiphysis. A hole was drilled into the medullary cavity with a 30-gauge needle (Mediq Denmark A/S, Brondby, Denmark) and 10μL D-PBS containing cancer cells were inoculated with a 0.3-mL insulin syringe (Terumo Medical Corporation, Terumo, Herlev, Denmark). The hole was closed with surgical Ethicon bone wax (Mediq Denmark A/S, Brondby, Denmark) and thoroughly irrigated with sterile saline. The skin was sutured with 4–0 Ethicon Vicryl rapid suture (V2920H, Mediq Denmark A/S, Brondby, Denmark), and a local anaesthetic was applied to the wound (Xylocain gel, 2.0% [w/v]; AstraZeneca, Albertslund, Denmark). Sham-operated controls underwent the same operation but were inoculated with D-PBS alone. Bone cancer was induced in BALB/cJ mice by inoculation of 10^4 4T1 cancer cells, and in C3H/HeN mice by inoculation of 10^5 NCTC 2472 cancer cells.

2.6. Spared nerve injury

The spared nerve injury was performed according to the method described by Decosterd and Woolf [13] In brief, mice were anaesthetized with hypnorm/dormicum. An incision was made in the skin at the mid thigh, and a section was made through the biceps femoris muscle to expose the 3 terminal branches of the sciatic nerve. The tibial and common peroneal branch were ligated with an Ethicon 8–0 virgin silk nonabsorbable suture (V120G, Mediq Denmark A/S, Brondby, Denmark) and cut approximately 1 to 2mm distal to the ligation. The muscle and skin were closed in 2 layers with 6–0 Dexon S adsorbable polyglycolic acid suture (Mediq Denmark A/S, Brondby, Denmark), and local anaesthetic was applied to the wound (Xylocain gel, 2.0% [w/v]; AstraZeneca, Albertslund, Denmark). Sham-operated controls were handled similarly, with exposure of the sciatic nerve and its branches but without contact to the nerve.

2.7. Formalin-induced pain

The formalin test was performed as described by Hunskaar et al. [30] with a few modifications. A 20-μL quantity of 2.5% (v/v) formalin in 0.9% sterile saline was injected subcutaneously into the plantar surface of the right hind paw with a GASTIGHT 50-μL microsyringe (Hamilton Co., VWR, Denmark) equipped with a $3^{½}$-gauge needle.

2.8. Behavioural tests

Limb use and weight bearing were assessed in sham and cancer operated mice. The tests were performed in sequence in the same animal always starting with the limb use test. Limb use was determined in an open field test that allowed the mouse to move freely about in a transparent standard cage without bedding (125×266×185mm; Tecniplast polycarbonate, Scanbur A/S, Karlslunde, Denmark). The gait of the affected limb were, after 3 minutes of motion, assigned a limb use score on a scale from 4 to 0, where 4=normal use, 3=minor limping, 2=substantial limping, 1=substantial limping and partial lack of use, and 0=complete lack of use. Weight bearing was performed on a TSE Powermeter (TSE Systems GmbH, DE, Bad Homburg, Germany). Briefly, the mouse was allowed to step onto the scales and the individual load of the hind limbs were measured for 10 seconds. Three sequential measures were performed, and the mouse was forced to change position before each measurement. The weight-bearing ratio was calculated as weight placed on right hind limb divided by total weight on hind limbs. The average ratio from the 3 measurements were calculated and subjected to data analysis.

Mechanical allodynia and thermal hyperalgesia were assessed in sham-operated and spared nerve injury-operated mice. The mice were allowed to habituate in individual red toned cylinder cages (inside diameter 7cm, height 7cm; Scanbur A/S, Karlslunde, Denmark) placed on either a wired mesh or a glass surface approximately 30 minutes before each test. Mechanical allodynia was assessed with von Frey monofilaments (Stoelting, Wood Dale, Illinois, USA).

Monofilaments were applied perpendicular to the sural surface of the hind paw in ascending order (0.016–2.0g). A response was considered positive when the mouse withdrew its hind paw in 3 of 5 applications. Cutaneous hyperalgesia was determined in the Hargreaves test [26]. An infrared beam (193mW/cm^2, Hargreaves Apparatus, Ugo Basile, Comerio, Italy) was pointed at the plantar lateral surface of the hind paw and the latency to withdrawal of the paw measured. The test was performed in triplicate and the average latency subjected to data analysis.

The time spent licking and biting the injected paw was assessed in formalin injected mice. Each mouse was placed under a glass cylinder (1L, VWR, Herlev, Denmark) and allowed to habituate for 60 minutes. The mouse was then restrained, formalin was injected, and the mouse was immediately returned to the glass cylinder. The total time spent licking and biting the right hind paw was recorded to the nearest second in 5-minute blocks. The formalin response was divided into an early phase (0–10 minutes) and a late phase (10–60 minutes), and the accumulated time spent licking and biting in each phase was subjected to data analysis.

2.9. Tissue processing

BALB/cJ WT and P2X7R KO mice were processed for histochemical analysis day 14 postoperation. Mice were anaesthetized with Zoletil Mix 50 (Pharmacy Services, Faculty of Life Sciences, Frederiksberg, Denmark; zolazepam 25mg/mL, tiletamin 25mg/mL, xylazin 20mg/mL and butorphanol 10mg/mL; 2μL/g) and perfused intracardially with 12mL D-PBS

followed by 40mL 4% paraformaldehyde in D-PBS (PFA). Spinal cord segment L4 was removed dorsal to vertebrae L1–L2, postfixed in 4% PFA, cryoprotected overnight in 30% sucrose, and embedded in Tissue-Tek O.C.T. compound (Sakura Finetek, Copenhagen, Denmark) by rapid freezing in a bath of ethanol cooled in dry ice. Segments were stored at −80°C until sectioning.

The right femur and upper tibia were removed and stored in 4% PFA until micro computed tomography (μCT) had been completed. Bones were then decalcified in 12.5% EDTA solution (VWR, Herlev, Denmark, Titriplex III, pH 7.4, 4°C) for 3weeks and embedded in paraffin.

2.10. Immunohistochemistry

Spinal cord tissue was cut into 30-μm sections on a cryostat (Leica CM 3050 S; Leica Microsystems A/S, Herlev, Denmark) and stained as free-floating sections. The sections were thoroughly washed in 0.1% Triton X-100 in D-PBS (T-PBS) to remove Tissue-Tek O.C.T. compound followed by 1 hour incubation in T-PBS at RT. Sections were blocked 2 hours in 2% bovine serum albumin (BSA) in T-PBS at RT, washed 3×5 minutes in T-PBS and incubated with primary antibody. Sections were distributed evenly and stained with either antibody raised in rabbit against glial fibrillary acidic protein (GFAP; DakoCytomation, Glostrup, Denmark, Z0334, 1:500 in 2% BSA in T-PBS) or Iba 1 (Wako Pure Chemical Industries Ltd, Osaka, Japan; 019–19741, 1:300 in 2% BSA in T-PBS) overnight at 4°C. Sections were washed 3×5 minutes in T-PBS and then incubated 2 hours at RT with Alexa Fluor 594 goat anti-rabbit IgG (Molecular Probes, Invitrogen, Taastrup, Denmark; A3 631 1:300 in 2% BSA in T-PBS). After a final 3×5 minute wash in D-PBS, sections were mounted on SuperFrost microscope slides (Menzel Glaser, VWR, Herlev, Denmark) with Crystal Mount (Sigma-Aldrich, Brondby, Denmark). Stained sections were visualized with a Zeiss Axiskop 2 (Carl Zeiss MicroImaging GmbH, DE, Göttingen, Germany).

Activation of microglia and astrocytes were investigated in designated sham-operated and bone cancer-bearing BALB/cJ mice inoculated with 4T1 mammary cancer cells (n=8 and n=6, respectively). Only cancer-bearing mice with a limb use score ≤3 were included in the experiment. Astrocyte activation was quantified by densitometry as the ratio of ipsilateral to contralateral fluorescent GFAP immunoreactivity of the dorsal horn gray matter. Microglia activation was quantified as the number of Iba1-positive cells found in a predetermined area of 200×300μm^2 in the ipsilateral laminae I–IV. Three randomly selected sections were analyzed from each mouse, and the average ratios were subjected to statistical analysis. In addition, glial activation was investigated in spinal cord sections from sham-operated and cancer-bearing BALB/cJ WT and P2X7R KO mice. Three mice were included in each group, and approximately 10 sections from each mouse were visually inspected. Spinal cord tissue from cancer-bearing C3H/HeN mice, known to exhibit increased GFAP staining intensity [7,25,29], was included as a positive control.

2.11. Micro computed tomography

Distal femoral bones from BALB/cJ WT and P2X7R KO mice were scanned with a high-resolution micro computed tomography (μCT) system (vivaCT 40, Scanco Medical AG, Brüttisellen, Switzerland). The scan resulted in a 3-dimensional (3D) reconstruction of cubic voxel sizes of $10\times10\times10\mu m^3$. Each 3D image dataset consisted of approximately 210 μCT slide images of which 100 slide images (1050μm) were used for analysis of bone tissues (2048×2048pixels) with 16-bit gray levels. The 10-mm length volume of interest was defined as starting 0.5mm proximal to the subchondral bone plate of the distal femoral condyles and extending 10mm proximal along the femur. From accurately segmented μCT image datasets, all microarchitectural properties of the distal femur were calculated using true, unbiased and assumption-free 3D methods. Based on the above defined volume of interest, total volume (TV) was calculated as total specimen volume including bone and marrow within volume of interest, and bone volume fraction (BV/TV) as bone volume per total specimen volume. Bone surface to bone volume ratio (BS/BV), trabecular number (TbN), trabecular thickness (TbTh) and trabecular separation (TbSp) were also computed [15] From 3D μCT reconstruction images, the appearance of tumour-induced bone damage was observed and qualitative described.

2.12. Bone histology

Paraffin-embedded bones were cut longitudinal in 5-μm consecutive sections with a rotation microtome (HM 355 S, Brock and Michelsen, Birkerod, Denmark), fastened on SuperFrost Plus microscope slides (Menzel Glaser, VWR, Herlev, Denmark) and dried overnight at 37°C. Sections were stained with hematoxylin and eosin following standard procedure and evaluated microscopically to identify morphological changes and determine tumour burden. Digital images were obtained with a Olympus BX 51 microscope fitted with a ColorView Soft Imaging System (Olympus, Tokyo, Japan). Tumour burden were divided into an intraosseous and extraosseous part delimited by the bone cortex or by a virtual line joining the remnants of the bone, in cases in which the bone had been partially resorped because of osteolysis [51]

2.13. Osteoclast culture

Osteoclast cultures were prepared from bone marrow cells isolated from BALB/cJ WT and P2X7R KO mice as described by Takeshita et al. [49]. Mice were killed by cervical dislocation. Tibiae and femora were removed and dissected free of adhering tissue. The epiphysis were cut off at both ends, and the marrow flushed out with MEM alpha medium (μ-MEM, Gibco Invitrogen, Taastrup, Denmark) using a 27-gauge needle. Cell suspension were centrifuged 10 minutes at 220g, washed twice in α-MEM supplemented with 1% antibiotic-antimycotic (Gibco Invitrogen, Taastrup, Denmark) and treated 15 minutes with PharmLyse (BD Biociences, Franklin Lakes, New Jersey, USA) to eliminate red blood cells. After centrifugation, the cells were washed in α-MEM supplemented with 1% antibiotic-antimycotic, and resuspended in culture medium (α-MEM, 1% antibiotic-antimycotic and 10% fetal bovine serum, Gibco Invitrogen, Taastrup, Denmark) enriched with 100ng/mL recombinant mouse macrophage colony-stimulating factor (M-CSF, R&D Systems,

Abingdon, United Kingdom). The cells were cultured in a 100mm suspension culture dish (Corning, Ithaca, New York, USA).

Day 3 cell cultures were vigorously washed with D-PBS and harvested with 0.02% EDTA in D-PBS. Cells were seeded at 50,000 cells/cm^2 in 35- and 60-mm culture dish well plate (Nunclon Δ Surface, Nunc, Denmark) and cultured in culture medium enriched with 20–40ng/mL recombinant mouse M-CSF and 5–10ng/mL recombinant mouse receptor activator of NF-KB ligand (RANKL, R&D Systems Europe Ltd, Abingdon, United Kingdom). Half of the culture medium was renewed after 2days of subculture, and the cells subcultured for a total of 5days. Cell cultures were harvested for RNA and protein extraction or stained for tartrate-resistant acid phosphatase (Acid Phosphatase Leukocyte Kit, Sigma-Aldrich, Brondby, Denmark) to check the purity of the osteoclasts. Osteoclasts were identified as TRAP-positive cells with 3 or more nuclei.

2.14. RT-PCR expression of P2X7(a) and P2X7(k) receptors

Total RNA was prepared from osteoclast cultures by RNeasy (Qiagen, Alameda, California, USA) and reverse transcribed using OligoT primers (Superscript III first strand synthesis system for RT-PCR, Invitrogen, Carlsbad, California, USA). RT-PCR was performed with forward primers specific to either mouse P2X7(a) (5′-GCCCGTGAGCCACTTATGC-3′) or mouse P2X7(k) (5′-GCCAGTGAGACATTTATGC-3′) and reverse primers specific to either exon 4 (5′-GGTCAGAAGAGCACTGTGC-3′) or exon 5 (5′-CCTTGTCTTGTCATATGGAAC-3′) [38]. The PCR were performed with Platinum Blue PCR SuperMix (Invitrogen, Carlsbad, California, USA) with the following conditions: initialization for 5 minutes at 94°C; 35 cycles of 94°C for 30 seconds, 55°C for 30 seconds, 72°C for 30 seconds, and finally elongation at 72°C for 7 minutes. PCR products were resolved by agarose gel electrophoresis and visualized by ethidium bromide staining.

2.15. Western blot analysis of P2X7 receptors in spinal cord and osteoclasts

Protein was isolated from spinal cord tissue and salivary glands from BALB/CJ WT and P2X7R KO mice, from C57BL/6 WT mice and from C57BL/6 P2X7R KO mice from Pfizer.

Mice were killed by cervical dislocation. Spinal cord segments dorsal to vertebrae T13–L2 were quickly removed and rapidly frozen in a round-bottomed tube placed in dry ice. Tissue was stored at −80°C until further processing. Spinal cord tissue was homogenized with an Ultra Turrax T10 basic fitted with dispersing element S10N-5G (IKA Werke GmbH, KG, DE, Staufen, Germany) in lysis buffer (4mM EDTA, 4mM EGTA, and 1mM DTT in phosphate buffer) supplemented with Protease Inhibitor Cocktail (Sigma-Aldrich, Brondby, Denmark). Salivary gland was in similar way processed, except the lysis buffer was supplemented with SigmaFAST Protease Inhibitor Cocktail Tablet (Sigma-Aldrich, Brondby, Denmark).

Osteoclasts cultures were vigorously washed with D-PBS and the plates placed on ice. Cells were lysed with lysis buffer (0.01mM EDTA, 4mM EGTA, 200mM Dl-Dithiothretiol in D-PBS) supplemented with Protease Inhibitor Cocktail (Sigma–Aldrich, Brondby, Denmark) and collected with a cell scraper.

Spinal cord homogenates and osteoclast cell suspensions were centrifuged at 4°C for 30 minutes at 1000*g*, and the supernatants were placed on ice or stored at −80°C until further processing. Protein concentration was determined by a Bradford 96-well plate assay (Bradford reagent, Sigma Aldrich, Brondby, Denmark) according to the manufacturer's description.

Protein extracts were supplemented with SDS reducing sample buffer and dithiothretiol (62.5mM Tris–HCl, 1% SDS, 10% glycerol and 20mM DTT) and boiled 10 minutes at 70°C. A 3- to 20-μg quantity of protein was loaded onto an 8% TEO-CI SDS Cassette gel (Pagegel Inc., Kem-En-Tec, Taastrup, Denmark) and separated in MOPS running buffer (Kem-En Tec, Taastrup, Denmark). Proteins were transferred to a PVDF membrane (Immobilon-P, Millipore, Copenhagen, Denmark; 2 hours at 200V) in transfer buffer (12.5mM Tris, 15% glycine, 1% SDS, and 20% methanol).

P2X7 protein and GAPDH protein (internal standard) was detected by immunoblotting. Briefly, the membrane was blocked 2 hours in blocking buffer at RT (5% nonfat dry milk and 0.1% Tween20 in PBS, T-PBS), washed in T-PBS and incubated with P2X7 receptor antibody (Alomone, Jerusalem, Israel, APR-004, 1:1000) and anti-GAPDH antibody (Sigma Aldrich, Brondby, Denmark, G9545, 1:10,000) in blocking buffer at 4°C overnight. After a wash in T-PBS the membrane was incubated 1 hour at RT with anti-rabbit IgG peroxidase antibody (Sigma-Aldrich, Brondby, A-9169; 1:1800 in blocking solution). Finally, the membrane was washed in T-PBS and proteins were visualized with Pierce ECL Western Blotting substrate (VWR, Herlev, Denmark) according to the manufacturer's procedure. Images were acquired with the FluorChem HD2 or FluorChemQ (Alpha Innotech, Cell Biosciences, Santa Clara, California, USA).

2.16. Statistical analysis

Data are presented as mean±standard error of the mean. Statistical analysis was performed with GraphPad Prism (version 4.03 for Windows; GraphPad Software, San Diego, California, USA). Data was analysed with either two-way or one-way analysis of variance followed by Bonferroni or Newman–Keuls multiple comparison test, respectively. Limb use scores were evaluated at single time points with Kruskal–Wallis test followed by the Dunn multiple comparison test. The Student *t* test was performed as appropriate. For all statistical analyses, a probability value of <0.05 was considered significant.

3. Results

3.1. P2X7 receptor knockout mice were susceptible to bone cancer pain

BALB/cJ P2X7 receptor knockout (P2X7R KO) mice developed pain-related behaviours after induction of bone cancer. Moreover, in the cancer-bearing P2X7R KO mice the pain-related behaviours had an earlier onset and an apparently more severe pain phenotype as compared with the cancer-bearing WT mice.

The cancer-bearing P2X7R KO mice had significant decreased limb use score and weight-bearing ratio for the affected limb on both day 10 and 14 compared with the sham-operated P2X7R KO mice (day 10: 2.0±0.3 vs 3.5±0.2, $P<.001$ and 0.36±0.02 vs 0.46±0.01, $P<.001$,

respectively; day 14: 0.6±0.1 vs 4.0±0.0, $P<.001$ and 0.26±0.02 vs 0.46±0.01, $P<.001$, respectively. Fig. 1). Cancer-bearing WT mice had significant decreased limb use score and weight-bearing ratio only day 14 compared with the sham-operated WT mice (1.3±0.4 vs 3.9±0.1, $P<.01$ and 0.30±0.03 vs 0.49±0.02, $P<.001$, respectively. Fig. 1). No differences were found at any time between sham-operated P2X7R KO and sham-operated WT mice.

Subanalysis of day 14 limb use scores revealed that all cancer-bearing P2X7R KO mice had developed a limb use score ≤1. This was in contrast to the range of limb use scores obtained in the cancer-bearing WT mice, where also scores of 4, 3, and 2 were present.

The above finding is in contrast to what was found in models of inflammatory and neuropathic pain using P2X7R KO mice of C57BL/6 strain [5]. To investigate whether the background strain could account for the different outcome, we investigated whether pain-related behaviours were attenuated in a model of spared nerve injury induced neuropathic pain in the BALB/cJ P2X7R KO mice.

3.2. BALB/cJ P2X7 receptor knockout mice did not develop pain-related behaviours in a model of neuropathic pain

The BALB/cJ P2X7R KO mice did not develop mechanical allodynia or thermal hyperalgesia in the spared nerve injury (SNI) model of neuropathic pain.

SNI-operated P2X7R KO mice had mechanical thresholds comparable to both sham-operated P2X7R KO and WT mice indicating that mechanical allodynia had not developed. SNI-operated WT mice, as expected, exhibited a significant lowered mechanical threshold on days 2, 6, 9, 12, and 21 postoperation compared with the sham-operated WT mice. Also, SNI-operated WT mice had, on all days postoperation (except day 1), a significant lowered mechanical threshold compared with SNI-operated P2X7R KO mice (Fig. 2).

The same was generally observed in the Hargreaves test for thermal hyperalgesia. However, a significant different latency was found only between SNI-operated WT and P2X7R KO mice on days 6 and 16 postoperation ($P<.05$ and $P<.01$, respectively) (Fig. 2).

3.3. Bone degradation, tumour burden, and glial activation in wild-type and P2X7R knockout mice

Increased bone degradation was evident in both cancer-bearing BALB/cJ WT and cancer-bearing P2X7R KO mice. Bone integrity was assessed by μCT scanning; cancer-bearing BALB/cJ WT and P2X7R KO mice had significantly increased bone surface to bone volume ratio, decreased trabecular thickness, decreased trabebular number, and increased trabecular separation compared with the corresponding sham-operated mice (Fig. 3). However, no difference between cancer-bearing BALB/cJ WT and cancer-bearing P2X7R KO mice were observed for these parameters. Total specimen volume was significantly increased in both cancer-bearing P2X7R KO and WT mice as compared with the corresponding sham-operated mice (4.48±0.38mm^3 vs 3.10±0.06 mm^3 and 4.13±0.20mm^3 vs 3.38±0.14mm^3; $P<.01$ and $P<.001$, respectively) (Fig. 3). The total specimen volume in the cancer-bearing P2X7R KO mice was significantly larger than in the WT cancer-bearing mice ($P<.05$), possibly indicating a greater scattering of bone in the P2X7R KO mice. However, the

significance of this finding is uncertain, as no differences were found between cancer-bearing P2X7R KO and WT mice in any other bone parameter measured.

Visual inspection of the morphological changes in hematoxylin and eosin (H&E)-stained bone sections revealed no apparent difference between cancer-bearing WT and P2X7R KO mice. Bone degradation and osteoclastic resorption pits were evident. Moreover, new bone formation was found extracortically in both groups of cancer-bearing mice (Fig. 4).

Glial activation was investigated in sham-operated and cancer-bearing BALB/cJ mice. No difference was found in GFAP immunoreactivity or numbers of Iba1-positive cells between sham-operated and cancer-bearing mice (1.03±0.07 vs 1.13±0.06, P=.28, and 13.5±1.2 vs 14.8±0.4, P=.35, respectively), and thus there were no significant astrocyte or microglia activation (Fig. 5). Examination of glial activation in a subgroup of sham-operated and cancer-bearing BALB/cJ WT and P2X7R KO mice resulted in the same finding (data not shown). As a positive control increased GFAP immunoreactivity was seen in spinal cord tissue from cancer-bearing C3H/HeN mice (Fig. 5c).

3.4. P2X7 receptor antagonist A-438079 did not alleviate bone cancer pain

The effect of the P2X7 receptor antagonist A-438079 was investigated in a model of bone cancer pain without activation of microglia and astrocytes (BALB/cJ), and in a model with strong activation of astrocytes but no microglia activation (c3H/HeN). Acute A-438079 treatment (300μmol/kg, s.c.) had no effect on pain-related behaviours in either cancer-bearing BALB/cJ or C3H/HeN mice.

The cancer-bearing mice were designated for treatment with either A-438079 or vehicle. The cancer-bearing mice had, on day 14 and before drug administration, a significant decreased limb use score and weight-bearing ratio compared with sham-operated control mice, indicating bone cancer pain (BALB/cJ mice: limb use 2.0±0.4 and 2.0±0.4 vs 3.8±0.1, $P<.001$; weight-bearing 0.28±0.04 and 0.32±0.04 vs 0.49±0.01, $P<.001$. C3H/HeN mice: limb use 1.9±0.2 and 2.0±0.3 vs 4.0±0.0, $P<.001$; weight-bearing 0.42±0.03 and 0.33±0.01 vs 0.52±0.03, $P<.05$ and 0.001) (Fig. 6). Treatment with A-438079 did not improve limb use score or weight-bearing ratio in the cancer-bearing mice 30 or 60 minutes after drug administration when compared with vehicle-treated cancer-bearing mice (Fig. 6).

A-438079 (300μmol/kg, s.c.), at 30 minutes postadministration, had no effect on time to fall or acceleration at fall (139.5±29.3 s vs 197.5±18.4 s and 20.7±3.5rpm vs 27.7±2.2rpm, respectively) in a Rotarod challenge, and thus no apparently adverse effect on motor coordination in naive mice.

3.5. A-438079 treatment attenuated formalin-induced pain

To ensure that A-438079 was efficacious in mice the drug was tested in a model of formalin-induced pain, where A-438079 in rats previously had proved effective [34].

A-438079 (300μmol/kg, s.c.) significantly attenuated formalin-induced pain. A significant decrease in the accumulated time of biting and licking were seen in both the early phase (44.0±1.7 seconds vs 75.2±4.5 seconds; Fig. 7) and the late phase (75.9±23.3 seconds vs

138.4±11.9 seconds) 30 minutes after drug administration when compared with vehicle-treated mice.

3.6. Expression of the P2X7 receptor splice variants

Western blot confirmed that the P2X7 receptor was expressed at the protein level in spinal cord tissue. SDS-PAGE and immunoblotting revealed a single band of about 77kDa, which is consistent with the glycosylated form of the P2X7 receptor [38]. Expression of P2X7 receptors was seen in the spinal cord of both BALB/cJ P2X7R KO mice and C57BL/6 P2X7R KO mice from Pfizer. Because of a lack of antibody specificity, it is not possible to discriminate between the P2X7(a) or the P2X7(k) receptor [38]. However, the BALB/cJ P2X7R KO mice exhibited a stronger band than the C57BL/6 P2X7R KO mice from Pfizer, which could indicate the presence of the P2X7(k) receptor (Fig. 8). Densitometry of signal intensities from the housekeeping protein GAPDH verified that equal amounts of protein were loaded onto the gel.

As previously reported [38], no expression of the P2X7 receptor was seen in the salivary gland of P2X7R KO mice from Pfizer, confirming the specificity of the antibody (data not shown).

P2X7(a) and P2X7(k) splice variant receptor mRNA was expressed in osteoclasts from BALB/cJ WT mice (Fig. 8). Western blot confirmed the expression of P2X7R protein in osteoclasts from BALB/cJ WT mice where a clear band was seen at approximately 77kDa. However, no band was detected in the osteoclasts from BALB/cJ P2X7R KO mice (Fig. 8). Bands for the housekeeping protein GAPDH was seen in both BALB/cJ WT and P2X7R KO mice.

4. Discussion

The P2X7 receptor has been hypothesized to be part of a common pathway in the central sensitization seen in chronic pain, and treatment with selective P2X7 receptor antagonists attenuated pain-related behaviours in animal models of inflammatory and neuropathic pain [27,28,34,37]. In agreement, Chessell et al. and the present results demonstrated that P2X7R KO mice had attenuated pain-related behaviours in models of neuropathic and inflammatory pain [5]. Surprisingly, in the present study we found that P2X7R KO mice were susceptible to bone cancer pain, and moreover the P2X7R KO mice had an earlier onset of pain-related behaviours compared with cancer-bearing WT mice. Also, acute treatment with A-438079, a selective P2X7 receptor antagonist, failed to alleviate bone cancer pain-related behaviours.

Although both inflammation and nerve damage is present in bone cancer pain [42], the neurochemical changes differ from those observed in inflammatory and neuropathic pain, suggesting that the nociceptive mechanism of bone cancer pain in part is distinct [7,22]. An absence of microglia activation is a characteristic of the spinal cord central sensitization seen in mouse models of bone cancer pain [25,29], whereas strong activation of astrocytes is reported in some models of bone cancer pain, and seem to be dependent on the background strain and the inoculated cancer cell line [43].

P2X7 receptor activation of macrophages have led to release of mature IL-1β [5,17,48], and it has been shown that LPS primed microglia release IL-1β in response to P2X7 receptor activation [4,6]. In a rat model of bone cancer pain, increased levels of spinal cord IL-1β were found to be localized with the astrocytic marker GFAP [53]; thus, the P2X7 receptor has been suggested to play an important role in glial–neuronal signalling, in which glial P2X7 receptor activation leads to release of mature IL-1β and subsequently other pronociceptive mediators [5,17,48]. The expression of P2X7 receptors in microglia has been established, while conflicting results about the expression of P2X7 receptors at the protein level in astrocytes have called in question the contribution of astrocytic P2X7 receptors to spinal cord pathology [12].

No spinal cord activation of either microglia or astrocytes was found in cancer-bearing BALB/cJ WT or P2X7R KO mice, and it was speculated that the lack of astrocyte activation could be the reason for the apparent unimportant role of P2X7 receptors in bone cancer pain. To investigate the astrocytic contribution of the P2X7 receptor mediated pain, the P2X7 receptor selective antagonist, A-438079, was tested in 2 different models of bone cancer pain: the BALB/cJ model and the thoroughly investigated C3H/HeN model, where NCTC 2472 osteosarcoma cells are inoculated into the medullary cavity. In the C3H/HeN model, a strong activation of astrocytes is present and the absence of microglia activation is observed [7,25,29,50]. No effect of A-438079 was seen in either model, indicating that the contribution of astrocytic P2X7 receptors to bone cancer pain is negligible. This is supported by the finding that phosphorylated p38 mitogen-activated protein kinase (p-p38 MAPK), which is phosphorylated downstream of P2X7 receptor activation, has been shown to colocalize with the microglial marker Iba1, but not the astrocytic marker GFAP [6].

Together the above findings indicate that the P2X7 receptor does not play a role in the central sensitization in models of bone cancer pain, which support the implication of a distinct mechanism of nociceptive signalling in bone cancer pain. However, the results have been complicated by the recent discovery of a P2X7 receptor splice variant, the P2X7(k) receptor.

Two strains of P2X7R KO mice have been described. These were generated by GlaxoSmithKline (GSK) and Pfizer, respectively [5,48]. The P2X7(a) receptor was knocked out in both strains, whereas the P2X7(k) receptor escaped deletion in the P2X7R KO mouse from GSK [38]. The present experiments are performed in BALB/cJ P2X7R KO mice generated from backcross of the original C57BL/6J P2X7R KO mouse from GSK. Western blot analysis revealed bands for the P2X7 receptor in both BALB/cJ WT and P2X7R KO mice. Band for the P2X7 receptor was also detected in the spinal cord of the P2X7R KO mice from Pfizer. This was expected as the existence of a P2X7-like receptor in the central nervous system has been described [45,47]. The BALB/cJ P2X7R KO mice exhibited a stronger band than the P2X7R KO mice from Pfizer, which suggest the presence of the P2X7(k) receptor. The specific role of the P2X7(k) receptor in nociceptive signalling is unknown; but it seems unlikely to fully undertake the role of the P2X7(a) receptor, as the GSK mouse was used to establish the role of the P2X7 receptor in inflammatory and neuropathic pain [5].

The P2X7R KO mice were not merely susceptible to bone cancer pain, they also had an earlier onset of pain-related behaviours, and seemingly a more severe pain phenotype compared with the cancer-bearing WT mice. A striking finding was that all cancer-bearing P2X7R KO mice in the last day of the study had developed a limb use score ≤1. This was in contrast to the broader range of limb use scores observed in the WT mice, which, in our experience, resembles the common observations in models of bone cancer pain. This finding led to the speculation that the BALB/cJ P2X7R KO mice were more susceptible to the pathology of the bone cancer than the WT mice.

P2X7 receptors are expressed in both osteoblasts and osteoclasts and have been found to be involved in normal physiological bone remodelling [18,20,32,33]. Therefore, it can be speculated that the P2X7 receptor deficiency leads to changes in the bone microenvironment. Recently, a polymorphism associated with loss of function in the P2X7 receptorwas linked to increased risk of fracture in postmenopausal women [40], supporting a role of P2X7 receptors in pathological bone degradation. The expression of the P2X7(a) and P2X7(k) receptor splice variants was investigated in osteoclasts isolated from BALB/cJ WT and P2X7R KO mice. P2X7 receptors were detected at the protein level in cultured osteoclast from WT mice but not in osteoclasts isolated from P2X7R KO mice, suggesting that an osteoclastic expression of the P2X7(k) splice variant receptor cannot explain the more severe pain-related behaviours in the cancer-bearing P2X7R KO mice. However, overall it is likely that the presence of the P2X7(k) receptor influences bone remodelling, as opposing differences was reported in the skeletal phenotype of the P2X7R KO mice from Pfizer and GSK [19,32].

The extent of bone cancer pain has been correlated to the extent of bone degradation in both humans and in animal models of bone cancer pain [2,24], and reduction of osteoclast activity by bisphosphonate treatment alleviates bone cancer pain [11,24,46]. Bone degradation was evident in both cancer-bearing WT and P2X7R KO mice. However, most of the parameters measured by μCT showed no difference in amount of bone loss between cancer-bearing WT and P2X7R KO mice. The only parameter that differed among the genotypes was a significant increase in the total specimen volume of the cancer-bearing femur in P2X7R KO mice compared with WT mice, indicating a greater scattering of the bone. However, the significance of this finding is uncertain. Also, no correlations could be found between the pain-related behaviours and any of the measured bone parameters. In the present study, the bone cancer had progressed to an advanced stage with excessive tumour burden and bone degradation; it is possible that this could have obscured any differences among the cancer-bearing WT and P2X7R KO mice, and that measurements at earlier time points could provide a different result.

The present data cannot provide a clear explanation why P2X7 receptor-deficient mice had more severe bone cancer pain-related behaviours compared with WT mice. We have discussed the lack of involvement of glial activation and the possible contribution of the bone microenvironment. Another explanation could be a difference in tumour burden. Increased levels of extracellular ATP have been found at tumour sites [41], and one could speculate that a different tumour burden in the cancer-bearing P2X7R KO mice compared with the cancer-bearing WT mice would result in different ATP release and thus different

stimulation of purinergic receptors. Apart from the P2X7 receptor other purinergic receptors have been implicated in pain signalling. Among these the P2X2/3 and P2X3 receptors have been suggested to be involved in bone cancer pain [21,23,31]. In the present study, excessive tumour burden was demonstrated by histology, however, it was not possible to obtain quantitative data.

In summary, we found that P2X7 receptor-deficient mice were susceptible to bone cancer pain and, moreover, had an earlier onset of pain-related behaviours compared with the cancer-bearing WT mice. These findings support the notion that bone cancer pain is a separate pain state. However, the purinergic involvement in bone cancer pain is complex, and further experiments are needed to elucidate how the earlier onset of pain-related behaviour is related to the deletion of the P2X7(a) receptor and the expression of the P2X7(k) receptor.

Acknowledgements

The research described in this paper was supported in part by The Danish Council of Independent Research, Medical Sciences; The Beckett Foundation, and *A.P. Møller og Hustru Chastine Mc-Kinney Møllers Fond til almene Formaal.* The C57BL/6 P2X7R KO mice were kindly provided by Ivana Novak, Faculty of Science, Copenhagen University, Copenhagen, Denmark.

References

[1]. Banning A, Sjogren P, Henriksen H. Treatment outcome in a multidisciplinary cancer pain clinic. Pain. 1991;47:129–134. [PubMed: 1762805]

[2]. Berruti A, Dogliotti L, Gorzegno G, Torta M, Tampellini M, Tucci M, Cerutti S, Frezet MM, Stivanello M, Sacchetto G, Angeli A. Differential patterns of bone turnover in relation to bone pain and disease extent in bone in cancer patients with skeletal metastases. Clin Chem. 1999;45:1240–1247. [PubMed: 10430790]

[3]. Burnstock G Purinergic receptors and pain. Curr Pharm Des. 2009;15:1717–1735. [PubMed: 19442186]

[4]. Chakfe Y, Seguin R, Antel JP, Morissette C, Malo D, Henderson D, Seguela P. ADP and AMP induce interleukin-1beta release from microglial cells through activation of ATP-primed P2X7 receptor channels. J Neurosci. 2002;22:3061–3069. [PubMed: 11943809]

[5]. Chessell IP, Hatcher JP, Bountra C, Michel AD, Hughes JP, Green P, Egerton J, Murfin M, Richardson J, Peck WL, Grahames CB, Casula MA, Yiangou Y, Birch R, Anand P, Buell GN. Disruption of the P2X7 purinoceptor gene abolishes chronic inflammatory and neuropathic pain. Pain. 2005;114:386–396. [PubMed: 15777864]

[6]. Clark AK, Staniland AA, Marchand F, Kaan TK, McMahon SB, Malcangio M. P2X7-dependent release of interleukin-1beta and nociception in the spinal cord following lipopolysaccharide. J Neurosci. 2010;30:573–582. [PubMed: 20071520]

[7]. Clohisy DR, Mantyh PW. Bone cancer pain. Clin Orthop Relat Res. 2003;S279–S288. [PubMed: 14600620]

[8]. Clohisy DR, Ogilvie CM, Carpenter RJ, Ramnaraine ML. Localized, tumor-associated osteolysis involves the recruitment and activation of osteoclasts. J Orthop Res. 1996;14:2–6. [PubMed: 8618161]

[9]. Clohisy DR, Ogilvie CM, Ramnaraine ML. Tumor osteolysis in osteopetrotic mice. J Orthop Res. 1995;13:892–897. [PubMed: 8544026]

[10]. Coleman RE. Clinical features of metastatic bone disease and risk of skeletal morbidity. Clin Cancer Res. 2006;12:6243s–6249s. [PubMed: 17062708]

[11]. Costa L, Major PP. Effect of bisphosphonates on pain and quality of life in patients with bone metastases. Nat Clin Pract Oncol. 2009;6:163–174. [PubMed: 19190592]

[12]. Cotrina ML, Nedergaard M. Physiological and pathological functions of P2X7 receptor in the spinal cord. Purinergic Signal. 2009;5:223–232. [PubMed: 19205927]

[13]. Decosterd I, Woolf CJ. Spared nerve injury: an animal model of persistent peripheral neuropathic pain. Pain. 2000;87:149–158. [PubMed: 10924808]

[14]. Dinarello CA. The IL-1 family and inflammatory diseases. Clin Exp Rheumatol. 2002;20:S1–S13.

[15]. Ding M Microarchitectural adaptations in aging and osteoarthrotic subchondral bone tissues. Acta Orthopaedica. 2010;81:1–53.

[16]. Donnelly-Roberts D, McGaraughty S, Shieh CC, Honore P, Jarvis MF. Painful purinergic receptors. J Pharmacol Exp Ther. 2008;324:409–415. [PubMed: 18042830]

[17]. Ferrari D, Pizzirani C, Adinolfi E, Lemoli RM, Curti A, Idzko M, Panther E, Di Virgilio F. The P2X7 receptor: a key player in IL-1 processing and release. J Immunol. 2006;176:3877–3883. [PubMed: 16547218]

[18]. Gartland A, Buckley KA, Hipskind RA, Bowler WB, Gallagher JA. P2 receptors in bone—modulation of osteoclast formation and activity via P2X7 activation. Crit Rev Eukaryot Gene Expr. 2003;13:237–242. [PubMed: 14696970]

[19]. Gartland A, Buckley KA, Hipskind RA, Perry MJ, Tobias JH, Buell G, Chessell I, Bowler WB, Gallagher JA. Multinucleated osteoclast formation in vivo and in vitro by P2X7 receptor-deficient mice. Crit Rev Eukaryot Gene Expr. 2003;13:243–253. [PubMed: 14696971]

[20]. Gartland A, Hipskind RA, Gallagher JA, Bowler WB. Expression of a P2X7 receptor by a subpopulation of human osteoblasts. J Bone Miner Res. 2001;16:846–856. [PubMed: 11341329]

[21]. Gilchrist LS, Cain DM, Harding-Rose C, Kov AN, Wendelschafer-Crabb G, Kennedy WR, Simone DA. Re-organization of P2X3 receptor localization on epidermal nerve fibers in a murine model of cancer pain. Brain Res. 2005;1044:197–205. [PubMed: 15885218]

[22]. Goblirsch MJ, Zwolak PP, Clohisy DR. Biology of bone cancer pain. Clin Cancer Res. 2006;12:6231s–6235s. [PubMed: 17062706]

[23]. Gonzalez-Rodriguez S, Pevida M, Roques BP, Fournie-Zaluski MC, Hidalgo A, Menendez L, Baamonde A. Involvement of enkephalins in the inhibition of osteosarcoma-induced thermal hyperalgesia evoked by the blockade of peripheral P2X3 receptors. Neurosci Lett. 2009;465:285–289. [PubMed: 19765404]

[24]. Hald A, Hansen RR, Thomsen MW, Ding M, Croucher PI, Gallagher O, Ebetino FH, Kassem M, Heegaard AM. Cancer-induced bone loss and associated pain-related behavior is reduced by risedronate but not its phosphonocarboxylate analog NE-10790. Int J Cancer. 2009;125:1177–1185. [PubMed: 19444917]

[25]. Hald A, Nedergaard S, Hansen RR, Ding M, Heegaard AM. Differential activation of spinal cord glial cells in murine models of neuropathic and cancer pain. Eur J Pain. 2009;13:138–145. [PubMed: 18499488]

[26]. Hargreaves K, Dubner R, Brown F, Flores C, Joris J. A new and sensitive method for measuring thermal nociception in cutaneous hyperalgesia. Pain. 1988;32:77–88. [PubMed: 3340425]

[27]. Honore P, Donnelly-Roberts D, Namovic M, Zhong C, Wade C, Chandran P, Zhu C, Carroll W, Perez-Medrano A, Iwakura Y, Jarvis MF. The antihyperalgesic activity of a selective P2X7 receptor antagonist, A-839977, is lost in IL-1alphabeta knockout mice. Behav Brain Res. 2009;204:77–81. [PubMed: 19464323]

[28]. Honore P, Donnelly-Roberts D, Namovic MT, Hsieh G, Zhu CZ, Mikusa JP, Hernandez G, Zhong C, Gauvin DM, Chandran P, Harris R, Medrano AP, Carroll W, Marsh K, Sullivan JP, Faltynek CR, Jarvis MF. A-740003 [N-(1-[1]-2,2-dimethylpropyl)-2-(3,4-dimethoxyphenyl)acetamide], a novel and selective P2X7 receptor antagonist, dose-dependently reduces neuropathic pain in the rat. J Pharmacol Exp Ther. 2006;319:1376–1385. [PubMed: 16982702]

[29]. Honore P, Rogers SD, Schwei MJ, Salak-Johnson JL, Luger NM, Sabino MC, Clohisy DR, Mantyh PW. Murine models of inflammatory, neuropathic and cancer pain each generates a unique set of neurochemical changes in the spinal cord and sensory neurons. Neuroscience. 2000;98:585–598. [PubMed: 10869852]

[30]. Hunskaar S, Fasmer OB, Hole K. Formalin test in mice, a useful technique for evaluating mild analgesics. J Neurosci Methods. 1985;14:69–76. [PubMed: 4033190]

[31]. Kaan TK, Yip PK, Patel S, Davies M, Marchand F, Cockayne DA, Nunn PA, Dickenson AH, Ford AP, Zhong Y, Malcangio M, McMahon SB. Systemic blockade of P2X3 and P2X2/3 receptors attenuates bone cancer pain behaviour in rats. Brain. 2010;133:2549–2564. [PubMed: 20802203]

[32]. Ke HZ, Qi H, Weidema AF, Zhang Q, Panupinthu N, Crawford DT, Grasser WA, Paralkar VM, Li M, Audoly LP, Gabel CA, Jee WS, Dixon SJ, Sims SM, Thompson DD. Deletion of the P2X7 nucleotide receptor reveals its regulatory roles in bone formation and resorption. Mol Endocrinol. 2003;17:1356–1367. [PubMed: 12677010]

[33]. Korock J, Sims SM, Dixon SJ. P2X7 nucleotide receptors act through two distinct mechanisms to regulate osteoclast survival. J Bon Miner Res. 2004;19:S418–S419.

[34]. McGaraughty S, Chu KL, Namovic MT, Donnelly-Roberts DL, Harris RR, Zhang XF, Shieh CC, Wismer CT, Zhu CZ, Gauvin DM, Fabiyi AC, Honore P, Gregg RJ, Kort ME, Nelson DW, Carroll WA, Marsh K, Faltynek CR, Jarvis MF. P2X7-related modulation of pathological nociception in rats. Neuroscience. 2007;146:1817–1828. [PubMed: 17478048]

[35]. Mercadante S Malignant bone pain: pathophysiology and treatment. Pain. 1997;69:1–18. [PubMed: 9060007]

[36]. Mercadante S, Portenoy RK. Opioid poorly-responsive cancer pain. Part 1: clinical considerations. J Pain Symptom Manage. 2001;21:144–150. [PubMed: 11226765]

[37]. Nelson DW, Sarris K, Kalvin DM, Namovic MT, Grayson G, Donnelly-Roberts DL, Harris R, Honore P, Jarvis MF, Faltynek CR, Carroll WA. Structure-activity relationship studies on N'-aryl carbohydrazide P2X7 antagonists. J Med Chem. 2008;51:3030–3034. [PubMed: 18438986]

[38]. Nicke A, Kuan YH, Masin M, Rettinger J, Marquez-Klaka B, Bender O, Gorecki DC, Murrell-Lagnado RD, Soto F. A functional P2X7 splice variant with an alternative transmembrane domain 1 escapes gene inactivation in P2X7 knock-out mice. J Biol Chem. 2009;284:25813–25822. [PubMed: 19546214]

[39]. North RA. Molecular physiology of P2X receptors. Physiol Rev. 2002;82:1013–1067. [PubMed: 12270951]

[40]. Ohlendorff SD, Tofteng CL, Jensen JE, Petersen S, Civitelli R, Fenger M, Abrahamsen B, Hermann AP, Eiken P, Jorgensen NR. Single nucleotide polymorphisms in the P2X7 gene are associated to fracture risk and to effect of estrogen treatment. Pharmacogenet Genomics. 2007;17:555–567. [PubMed: 17558311]

[41]. Pellegatti P, Raffaghello L, Bianchi G, Piccardi F, Pistoia V, Di VF. Increased level of extracellular ATP at tumor sites: in vivo imaging with plasma membrane luciferase. PLoS One. 2008;3:e2599. [PubMed: 18612415]

[42]. Peters CM, Ghilardi JR, Keyser CP, Kubota K, Lindsay TH, Luger NM, Mach DB, Schwei MJ, Sevcik MA, Mantyh PW. Tumor-induced injury of primary afferent sensory nerve fibers in bone cancer pain. Exp Neurol. 2005;193:85–100. [PubMed: 15817267]

[43]. Sabino MA, Luger NM, Mach DB, Rogers SD, Schwei MJ, Mantyh PW. Different tumors in bone each give rise to a distinct pattern of skeletal destruction, bone cancer-related pain behaviors and neurochemical changes in the central nervous system. Int J Cancer. 2003;104:550–558. [PubMed: 12594809]

[44]. Samad TA, Moore KA, Sapirstein A, Billet S, Allchorne A, Poole S, Bonventre JV, Woolf CJ. Interleukin-1beta-mediated induction of Cox-2 in the CNS contributes to inflammatory pain hypersensitivity. Nature. 2001;410:471–475. [PubMed: 11260714]

[45]. Sanchez-Nogueiro J, Marin-Garcia P, Miras-Portugal MT. Characterization of a functional P2X(7)-like receptor in cerebellar granule neurons from P2X(7) knockout mice. FEBS Lett. 2005;579:3783–3788. [PubMed: 15978588]

[46]. Sevcik MA, Luger NM, Mach DB, Sabino MA, Peters CM, Ghilardi JR, Schwei MJ, Rohrich H, De Felipe C, Kuskowski MA, Mantyh PW. Bone cancer pain: the effects of the bisphosphonate alendronate on pain, skeletal remodeling, tumor growth and tumor necrosis. Pain. 2004;111:169–180. [PubMed: 15327821]

[47]. Sim JA, Young MT, Sung HY, North RA, Surprenant A. Reanalysis of P2X7 receptor expression in rodent brain. J Neurosci. 2004;24:6307–6314. [PubMed: 15254086]

[48]. Solle M, Labasi J, Perregaux DG, Stam E, Petrushova N, Koller BH, Griffiths RJ, Gabel CA. Altered cytokine production in mice lacking P2X(7) receptors. J Biol Chem. 2001;276:125–132. [PubMed: 11016935]

[49]. Takeshita S, Kaji K, Kudo A. Identification and characterization of the new osteoclast progenitor with macrophage phenotypes being able to differentiate into mature osteoclasts. J Bone Miner Res. 2000;15:1477–1488. [PubMed: 10934646]

[50]. Trang T, Beggs S, Salter MW. Purinoceptors in microglia and neuropathic pain. Pflugers Arch. 2006;452:645–652. [PubMed: 16767466]

[51]. van der Pluijm G, Que I, Sijmons B, Buijs JT, Lowik CW, Wetterwald A, Thalmann GN, Papapoulos SE, Cecchini MG. Interference with the microenvironmental support impairs the de novo formation of bone metastases in vivo. Cancer Res. 2005;65:7682–7690. [PubMed: 16140935]

[52]. Zech DF, Grond S, Lynch J, Hertel D, Lehmann KA. Validation of World Health Organization Guidelines for cancer pain relief: a 10-year prospective study. Pain. 1995;63:65–76. [PubMed: 8577492]

[53]. Zhang RX, Liu B, Wang L, Ren K, Qiao JT, Berman BM, Lao L. Spinal glial activation in a new rat model of bone cancer painproduced by prostate cancer cell inoculation of the tibia. Pain. 2005;118:125–136. [PubMed: 16154703]

[54]. Zimmermann M Ethical guidelines for investigations of experimental pain in conscious animals. Pain. 1983;16:109–110. [PubMed: 6877845]

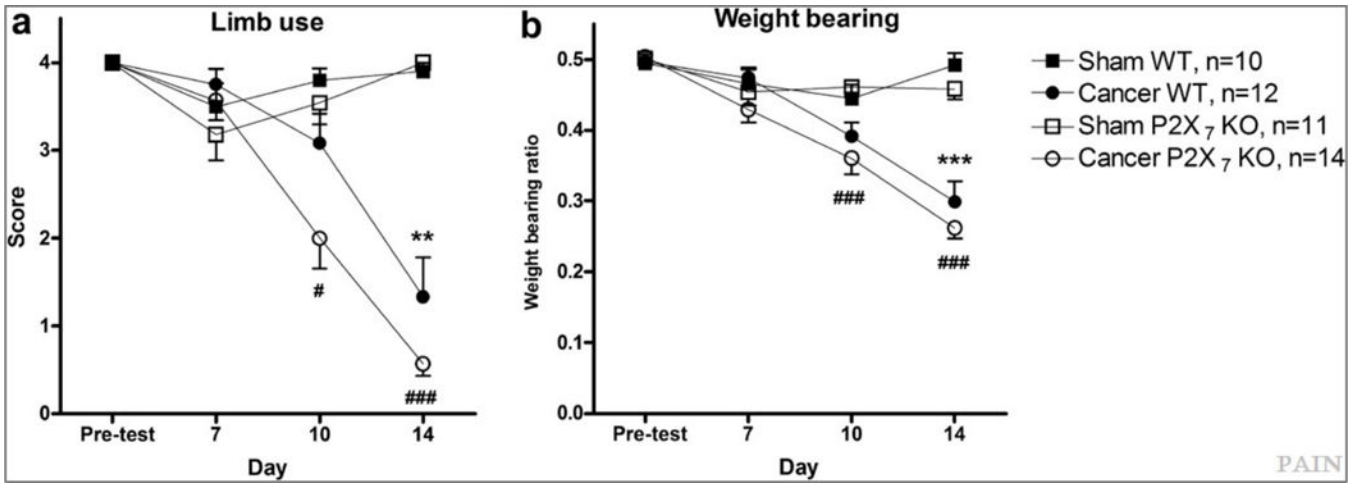

Fig. 1.

P2X7 receptor knockout mice were susceptible to bone cancer pain, and the pain-related behaviours had an earlier onset compared with wild-type mice. Cancer-bearing P2X7 receptor knockout mice exhibited, on days 10 and 14, a significant decreased limb use score (a) and weight-bearing ratio (b), whereas cancer-bearing wild-type mice exhibited this only on day 14. ***P < .001 and **P < .01 in cancer-bearing wild-type mice compared with sham-operated wild-type mice; ###P < .001 and #P < .05 in cancer-bearing P2X7 receptor knockout mice compared with sham-operated P2X7 receptor knockout mice.

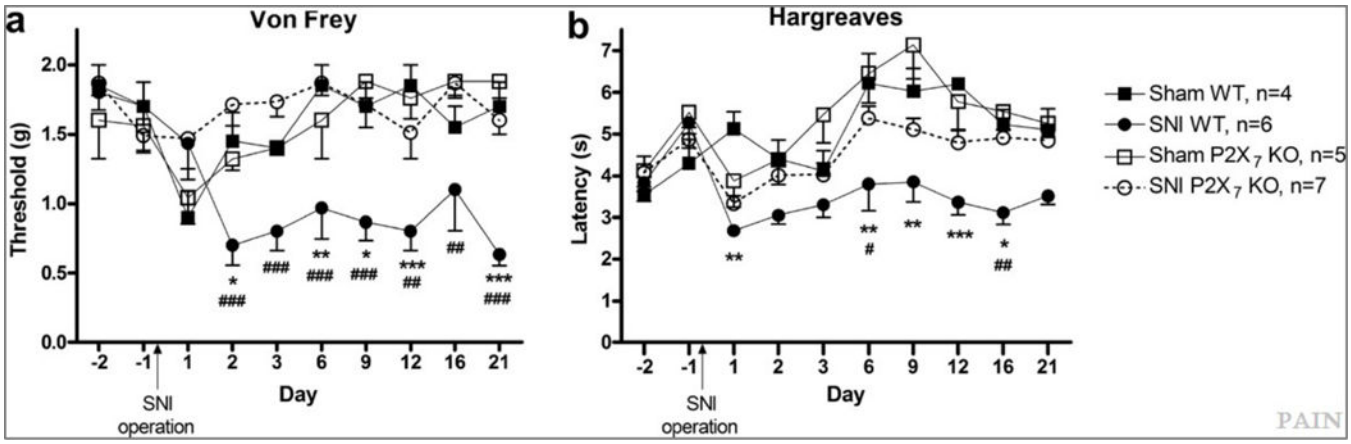

Fig. 2.

P2X7 receptor knockout mice did not develop pain-related behaviours in the spared nerve injury (SNI) model of neuropathic pain. (a) SNI-operated P2X7 receptor knockout mice exhibited no mechanical allodynia, while SNI-operated wild-type mice exhibited a significant lowered von Frey threshold after SNI operation compared with both sham-operated wild-type mice and SNI-operated P2X7 receptor knockout mice. (b) The same distribution was observed in the Hargreaves test for thermal hyperalgesia. ***P < .001, **P < .01, and *P < .05 in SNI-operated wild-type mice compared with sham-operated wild-type mice; ###P < .001, ##P < .01, and #P < .05 in SNI-operated wild-type mice compared with SNI-operated P2X7 receptor knockout mice.

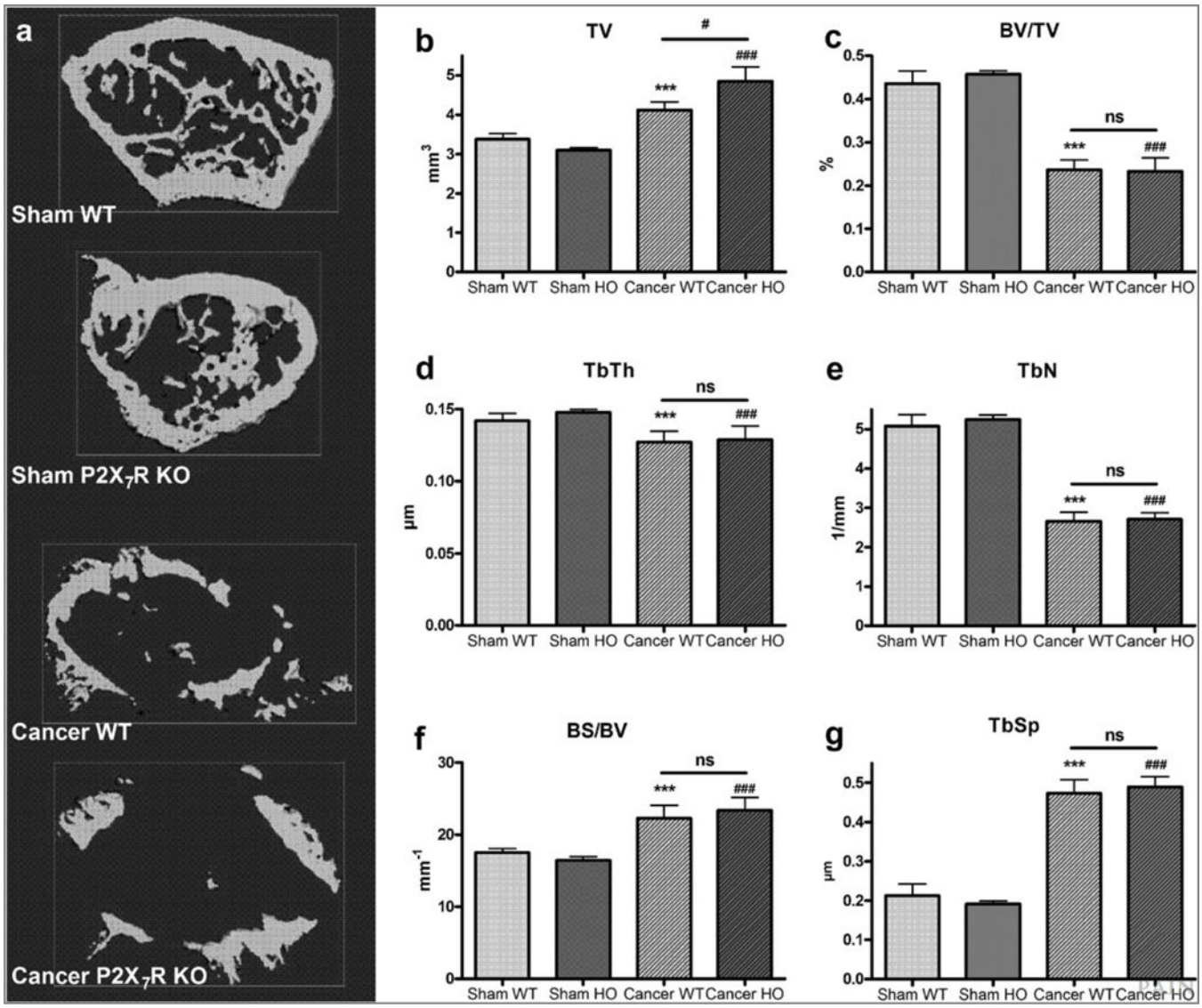

Fig. 3.

Micro computed tomography (µCT) analysis of femora from sham-operated and cancer-bearing wild-type and P2X7 receptor knockout mice. (a) Representative images of transverse sections from sham and cancer operated P2X7 receptor knockout and wild-type mice. (b) Total specimen volume in the cancer-bearing P2X7 receptor knockout mice was significantly larger than in the wild-type cancer-bearing mice. (c) Bone volume fraction. (d) Trabecular thickness. (e) Trabebular number. (f) Bone surface to bone volume ratio. (g) Trabecular separation. ***P < .001 in cancer operated wild-type mice compared with sham-operated wild-type mice; ###P < .001 in cancer operated P2X7 receptor knockout mice compared with sham-operated P2X7 receptor knockout mice; #P < .05; ns, Nonsignificant; n = 10–14 in each group.

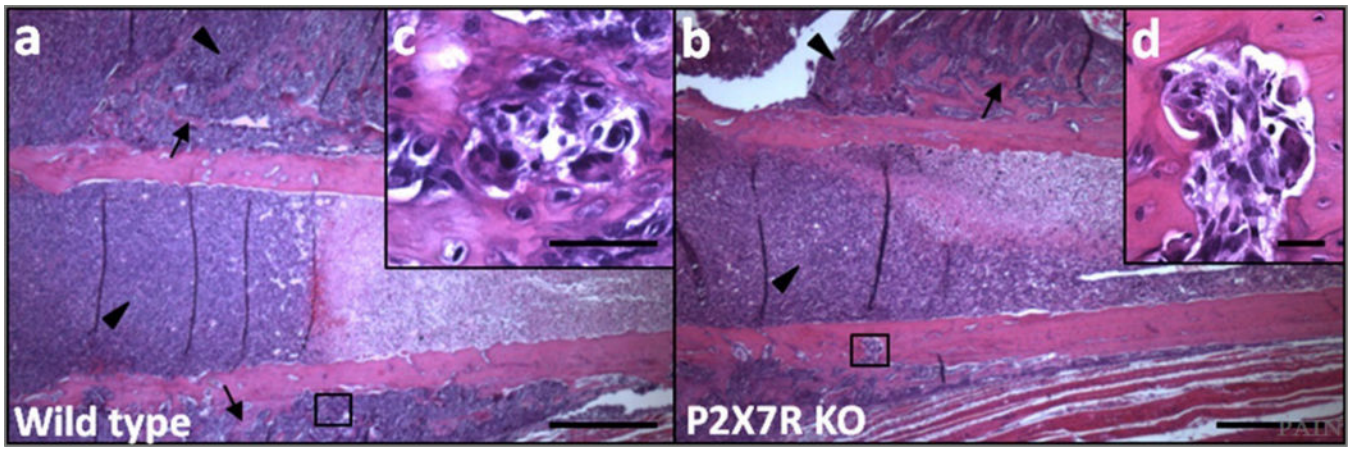

Fig. 4.

Representative images of haematoxylin and eosin stained femur sections from cancer-bearing BALB/cJ wild-type (a) and cancer-bearing P2X7 receptor knockout mice (b). The images show bone degradation, new bone formation, and tumour burden. (c) and (d) Insets from image (a) and (b), respectively, demonstrating zones of bone resorption. Arrowheads (★) designate tumour burden inside and outside of the bone. Arrows (→) designate new bone formation. Size scale 500 μm in (a and b) and 50 μm in (c and d).

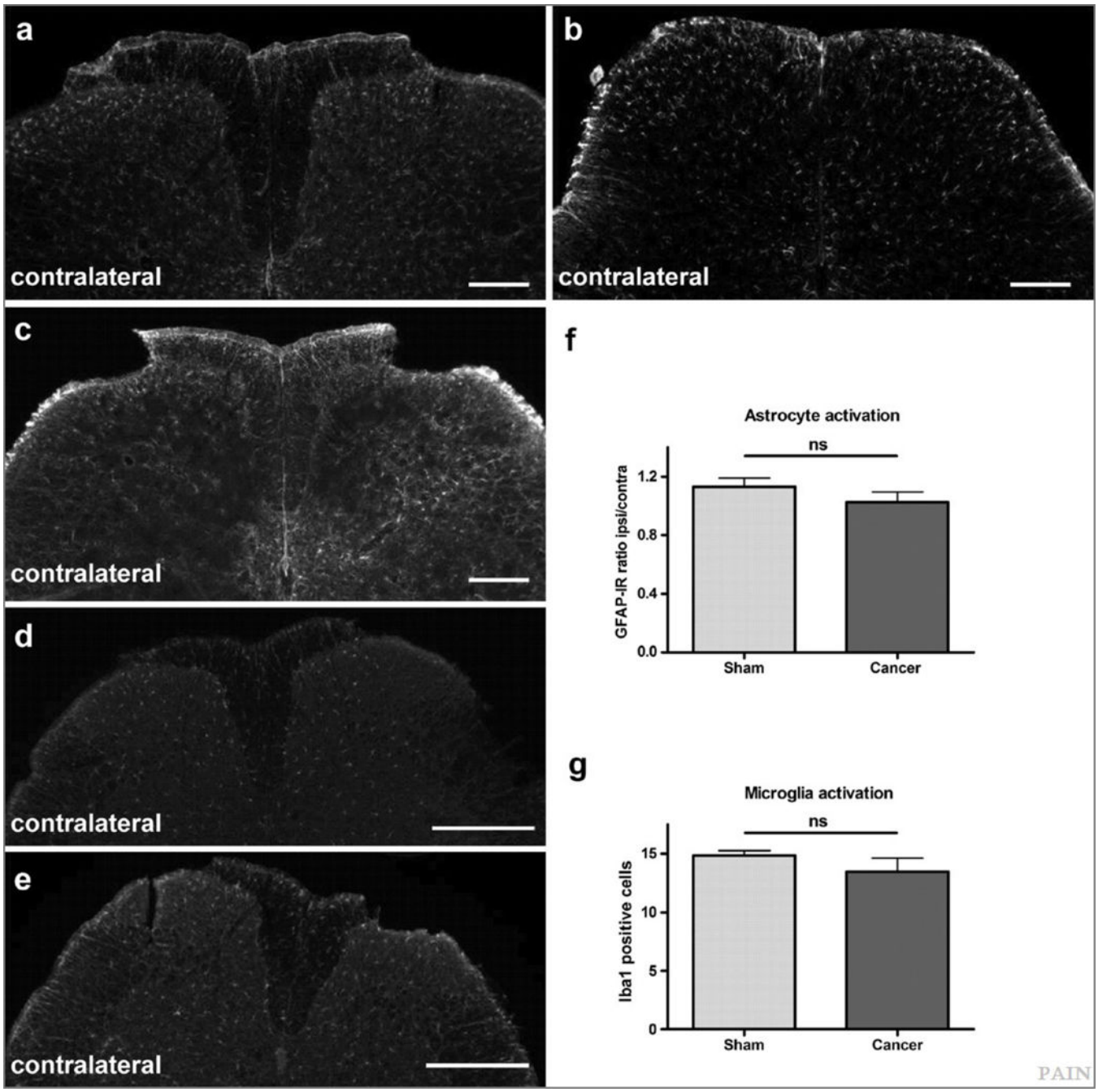

Fig. 5.

Cancer-bearing BALB/cJ mice inoculated with 4T1 mammary cancer cells showed no astrocyte or microglia activation in the dorsal horn of the spinal cord. GFAP spinal cord expression in the contralateral and ipsilateral dorsal horn of sham-operated (a) and cancer-bearing BALB/cJ mice (b). Increased GFAP spinal cord expression in the ipsilateral dorsal horn of cancer-bearing C3H mice inoculated with NCTC 2472 osteosarcoma cells (c). Iba1 spinal cord expression in the contralateral and ipsilateral dorsal horn of sham-operated (d) and cancer-bearing BALB/cJ mice (e). No significant change was found in the ratio of

ipsilateral to contralateral fluorescent GFAP immunoreactivity (f) or in the numbers of Iba1-positive cells found in a predetermined area of 200 × 300 μm2 in the ipsilateral laminae I–IV (g). For either sham-operated or and cancer-bearing BALB/cJ mice, respectively, n = 6 and n = 8. Three randomly selected sections were analyzed from each mouse and the average ratios subjected to statistical analysis ns, Nonsignificant. Scale, 200 μm.

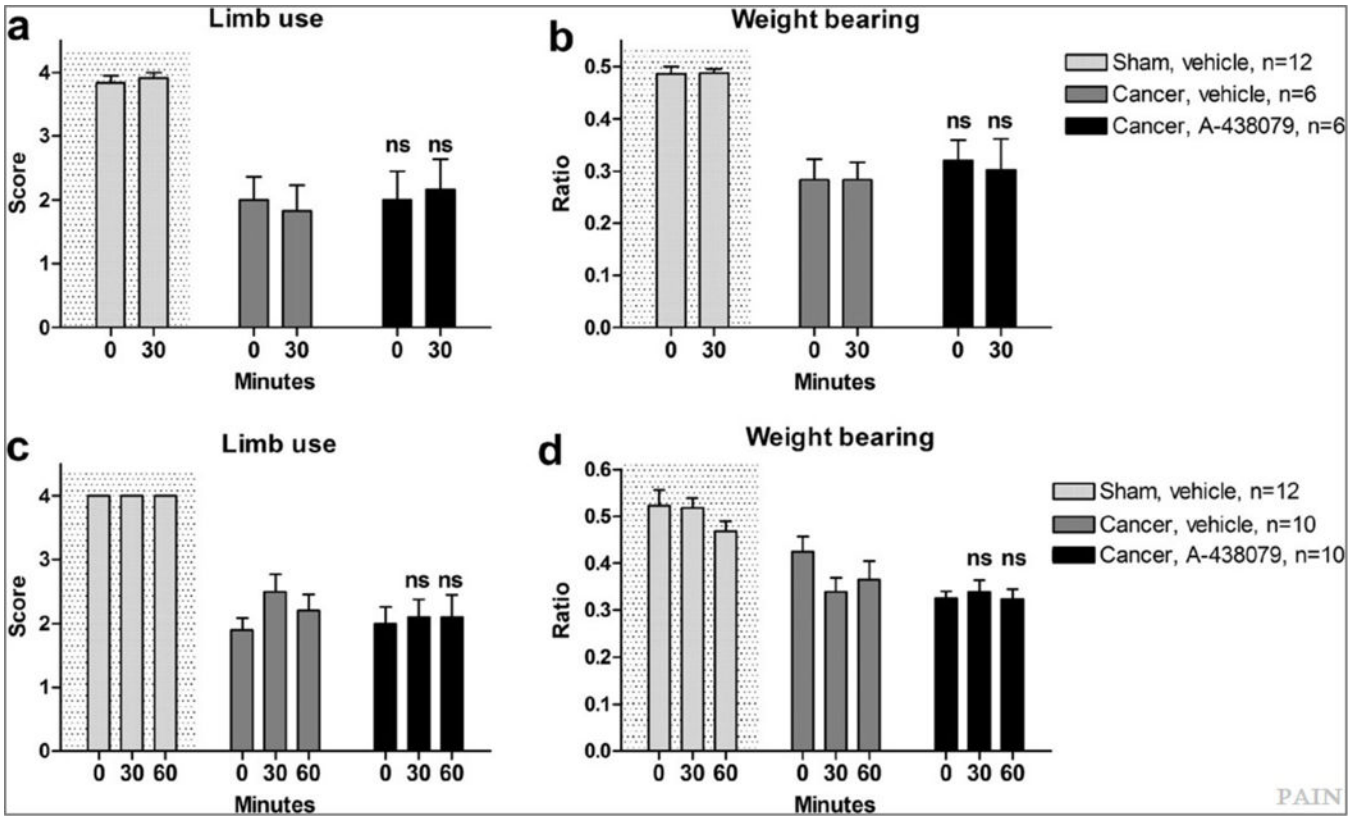

Fig. 6.

Acute treatment with A-438079 (300 μmol/kg, s.c.) had no effect on limb use score (a and c) or weight bearing (b and d) 30 or 60 minutes post administration in either cancer-bearing BALB/cJ (a and b) or cancer-bearing C3H/HeN mice (c and d). Both vehicle and A-438079-treated cancer-bearing mice showed pain-related behaviours compared with vehicle-treated sham-operated mice ($P < .01$ or $P < .001$). ns, Nonsignificant compared with vehicle-treated cancer-bearing mice at the same point of time.

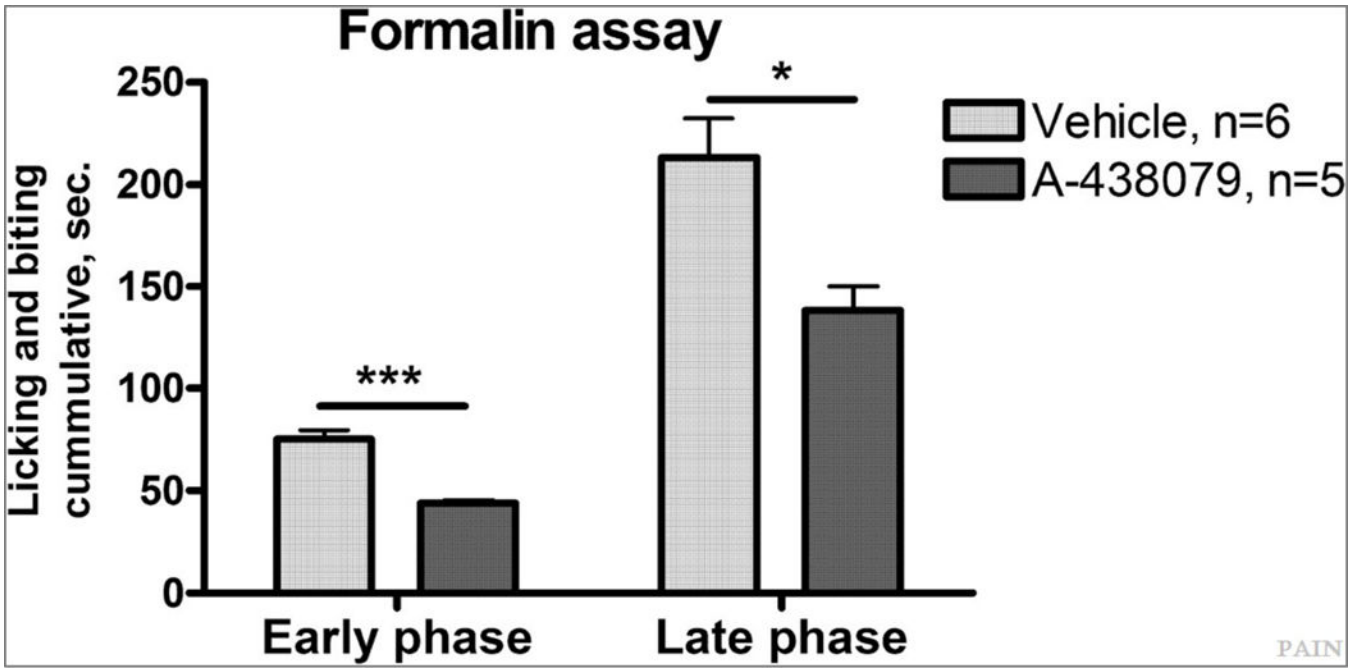

Fig. 7.

Acute treatment with A-438079 (300 μmol/kg, s.c.) significantly attenuated the nociceptive behaviours in the early phase (0–10 minutes) and the late phase (10–60 minutes) of formalin-induced pain. *P < .05, ***P < .001.

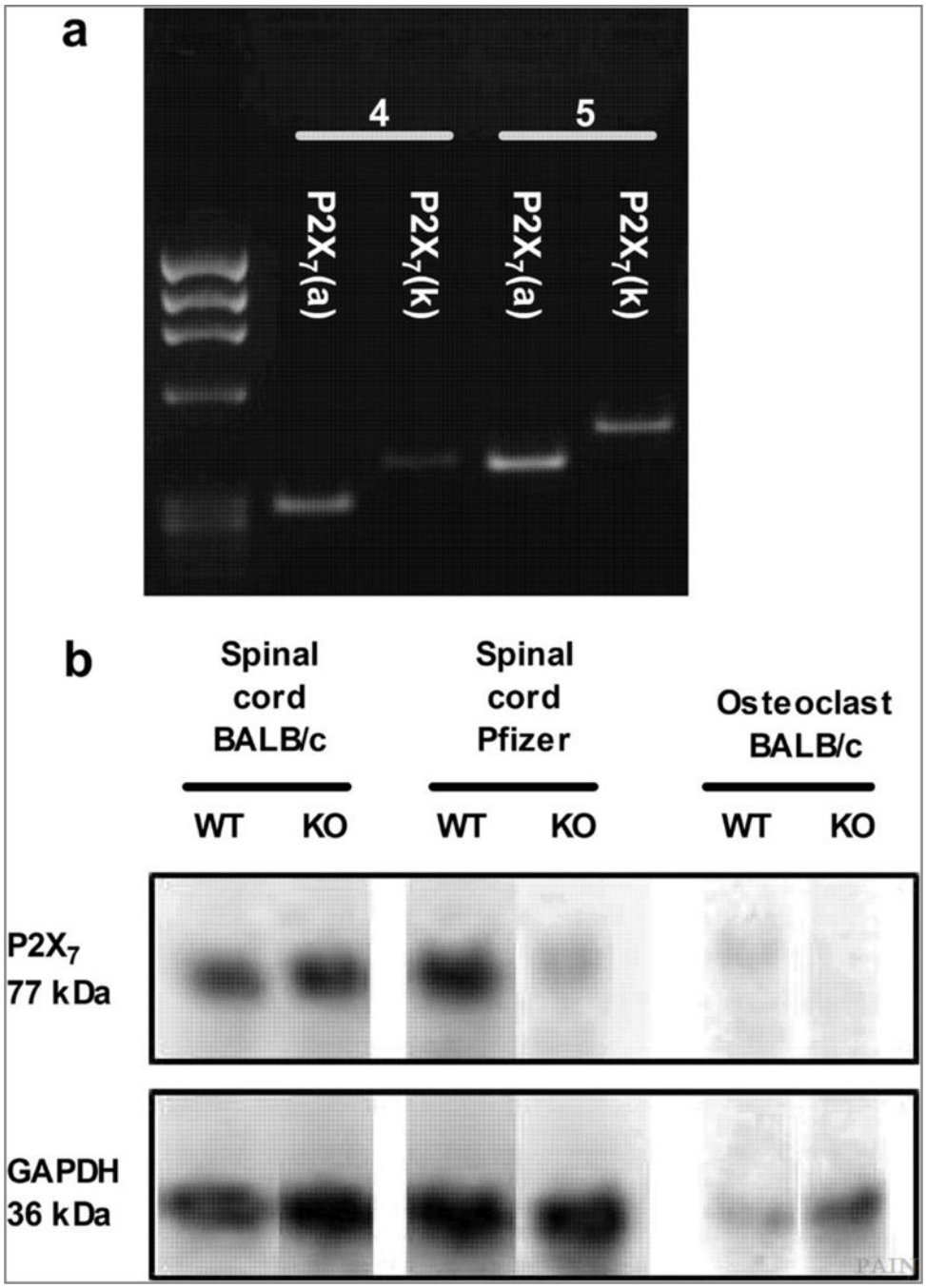

Fig. 8.

P2X7(a) and P2X7(k) receptor mRNA was expressed in BALB/cJ osteoclasts by RT-PCR (a). Forward primers specific to either mouse P2X7(a) or mouse P2X7(k) and reverse primers specific to either exon 4 or exon 5 were used. (b) P2X7 receptors were detected at the protein level in spinal cord of both BALB/cJ wild-type and P2X7 receptor knockout mice. Bands were also detected in spinal cord of P2X7 receptor knockout mice from Pfizer. In osteoclasts isolated from BALB/cJ wild-type mice the P2X7 receptor was expressed at the

protein level, while no expression was found in osteoclasts isolated from BALB/cJ P2X7 receptor knockout mice. GAPDH protein was co-detected to determine protein load.